PREPARED FOR THE U.S. DEPARTMENT OF ENERGY,
UNDER CONTRACT DE-AC02-76-CHO-3073

PPPL-2847
UC-426

PPPL-2847

PLASMA FLUXES TO SURFACES FOR AN OBLIQUE MAGNETIC FIELD

BY

C.S. PITCHER, P.C. STANGEBY, M.G. BELL, ET AL.

July, 1992

PPPL PRINCETON PLASMA PHYSICS LABORATORY

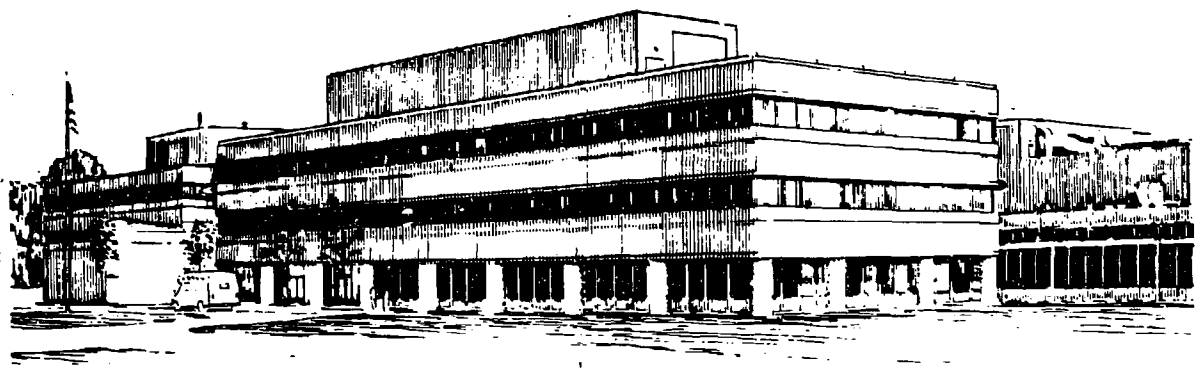

PRINCETON UNIVERSITY, PRINCETON, NEW JERSEY

PPPL--2847

DE92 018434

Paper Submitted to the 10th International Conference on Plasma-Surface Interactions in Controlled Fusion Devices, March 30 - April 3, 1992, Monterey, California, USA.

Plasma Fluxes to Surfaces for an Oblique Magnetic Field

C S Pitcher*, P C Stangeby**, M G Bell, J D Elder**, S J Kilpatrick, D M Manos, S S Medley, D K Owens, A T Ramsey and M Ulrickson

Princeton Plasma Physics Laboratory, Princeton University, Princeton, P.O. Box 451, NJ 08543, USA

* Canadian Fusion Fuels Technology Project, Toronto, Canada

** University of Toronto, Canada

Abstract

The poloidal and toroidal spatial distributions of D_α, He I and C II emission have been obtained in the vicinity of the TFTR bumper limiter and are compared with models of ion flow to the surface. The distributions are found not to agree with a model (the "Cosine" model) which determines the incident flux density using only the parallel fluxes in the scrape-off layer and the projected area of the surface perpendicular to the field lines. In particular, the Cosine model is not able to explain the significant fluxes observed at locations on the surface which are oblique to the magnetic field. It is further shown that these fluxes cannot be explained by the finite Larmor radius of impinging ions. Finally, it is demonstrated, with the use of Monte Carlo codes, that the distributions can be explained by including both parallel and cross-field transport onto the limiter surface.

1 Introduction

It is usually assumed in the design of magnetic fusion devices that the particle ϕ and power p flux densities incident on limiters or divertor plates are proportional to the product of the parallel field flux density in the scrape-off layer and the projected area perpendicular to the field lines, that is,

$$\phi \propto \phi_{par} \cos\theta \qquad [1]$$

$$p \propto p_{par} \cos\theta \qquad [2]$$

where θ is the angle between the surface normal and the magnetic field and "par" indicates parallel field fluxes [1]. These relationships, for the sake of brevity, may be called the "Cosine" law.

The Cosine law has lead to the use of glancing or oblique angles between the surface and the magnetic field to reduce power densities on critical first-wall components. In contemporary large, high-powered machines the parallel power densities flowing in the SOL can be very large, $> 100 MW m^{-2}$, and thus angles must be made very oblique to reduce the surface power density to an acceptable level, i.e. $|90-\theta| < 5°$. ITER extends this approach to $|90-\theta| \sim 2°$ [2].

In this paper we present new results from TFTR which indicate that the particle fluxes incident on the limiter, as deduced from the spatial distributions of D_α, He I and C II emissions, do not follow the Cosine law. The results are in agreement with a recent study on the DITE tokamak [3], which showed that the ion flux did not obey the Cosine law at oblique angles of incidence, i.e. for $|90-\theta| < 3°$, a condition which is satisfied for essentially all of the TFTR bumper limiter. It is demonstrated in the paper that the observed distributions can be explained by considering both parallel and cross-field transport of particles to the limiter.

In Section 2 we present the experimental arrangement, in Section 3 we compare the experimental results with the Cosine model, in Sections 4 and 5 we compare the experimental results with predictions from Monte Carlo modelling, in Section 6 we consider sputtering yields and finally in Sections 7 and 8 we discuss these results and conclude.

2 Experiment

The TFTR plasma cross-section is circular in shape with major and minor radii which were held constant in this experiment at $R_0 = 2.45m$ and $a = 0.80m$, respectively. The plasma is limited by a toroidal inner-wall bumper limiter composed of discrete graphite tiles covering an

area of $\sim 22m^2$, Fig. 1. The toroidal limiter has a periodic structure in the toroidal direction which repeats at each bay, see Fig. 2. There are 20 such bays equi-spaced around the torus, corresponding to the 20 toroidal field coils.

The limiter shape and pitch of the magnetic field in the SOL (typically ~4°) are such that, according to the Cosine law, the plasma-limiter interaction should be most intense in the upper left and low right quadrants of a given bay, as depicted in Fig. 2a. Conversely, the upper right and lower left quadrants should receive little in the way of particle and power fluxes due to the shadowing effect of adjacent bays. Similarly, the vertical centre of the bay should receive little particle flux since the field lines are approximately parallel to the surface. Thus, although the nominal area of the limiter is $\sim 22m^2$, because of the limiter's convoluted shape, the area that is expected to be in direct contact with the plasma (i.e. "wetted") is $\sim 5m^2$. These geometrical considerations are discussed in detail in [4,5].

The plasma boundary has been diagnosed in this study with a reciprocating Langmuir probe located approximately 37 cm above the outside midplane and a CCD camera plasma viewing periscope system (Bay P) which measures both the poloidal and toroidal distributions of visible emissions from low ionization states [6] In this study we shall concentrate on the spatial distributions of the following spectral lines, D_α, He I (587.6 nm) and C II (657.8 nm).

In the cases of the D_α and He I distributions, it is assumed that the surface is approximately in equilibrium, i.e. that the flux density of incident ions is approximately equal to the flux density of neutrals leaving the surface [7]. These species generally radiate within a few centimetres of their point of origin on the limiter surface, which is small compared to the bumper limiter dimensions (~ 1 m). In the plasma the neutrals radiate at a photon efficiency which is a weak function of the electron temperature in the case of D_α, somewhat stronger in the case of He I [8]. In general, the radial variation of the electron temperature in the boundary is weak [9] and therefore it is reasonable to assume that the photon efficiency across the limiter surface is a constant. Thus, the intensity distributions of D_α and He I are reasonable representations of the flux density of both the ionic bombardment of the limiter and the neutral influx. In the case of the C II emission, it can only be assumed that the emission distribution is representative of the influx, since the release mechanism is thought in TFTR to be due primarily to physical sputtering rather than recycling [9].

3 Cosine Model

Fig. 3a gives an intensity contour plot of the D_α emission for Bay P obtained with the camera above the mid-plane in a deuterium Ohmic discharge with $I_p = 1.4MA$, $B_T = 4T$ and $\bar{n}_e = 3x10^{19}m^{-3}$. Also shown for comparison are the corresponding particle flux density contours derived from the Cosine model (Fig. 3b) and contours of the angle of the magnetic field with the surface used in the model, i.e. $|90 - \theta|$ (Fig. 3c). The Cosine model takes into account the full three-dimensional shape of the limiter (including each tile) [4,5], the two-dimensional magnetic geometry and the parallel particle flux e-folding distance as measured by the reciprocating Langmuir probe. The probe measures $\lambda_\Gamma = 3.0cm$ at the outside mid-plane, which corresponds to a value of $\lambda_\Gamma = 5.0cm$ at the inside mid-plane, when the magnetic geometry is taken into account [9]. The model determines the spatial distribution of particle flux density onto the limiter surface taking in to account the "Cosine" law (Eqn. 1) and the shadowing effect of neighbouring bays. Field ripple is small at the inner wall in TFTR and has been neglected. The distributions obtained in the model have been smoothed to aid in their graphical display in Fig. 3.

As expected, the Cosine model produces a flux pattern which is concentrated in the upper left quadrant (this is reversed below the mid-plane so that the interaction is mainly with the lower right quadrant, not shown) with virtually no flux incident in the upper right quadrant (also lower left). This is primarily due to the shadowing effect of the adjacent bays. This is in sharp contrast with the experimental pattern which straddles the middle of the bay, Fig. 3a.

The vertical and horizontal flux variations are brought out more clearly in Fig. 4, which compares the experiment with the Cosine model. In the case of the vertical distributions (Fig. 4a), the patterns have been integrated in the horizontal direction whilst in the horizontal distribution (Fig. 4b), a horizontal intensity scan at z = 0.50 m has been used. The Cosine model predicts, in the case of the vertical distribution, a strong minimum at the midplane (z = 0.0 m) at a level of ~ 15% of the peak level, as approximately found from simpler, analytic models [10]. In striking contrast, the experiment shows a mid-plane signal which is approximately ~ 70% of the peak intensity. The model agrees reasonably well with the overall vertical width of the experimental distribution. The vertical width is determined primarily by the radial decay of the parallel field flux density.

In the case of the horizontal distribution (Fig. 4b), although the experiment and the Cosine model peak at approximately the same horizontal location (y ~ - 0.1 m), the experimental distribution extends well to the right of the middle of the bay, a region where the Cosine model

predicts is completely shadowed by an adjacent bay and thus should receive no particle flux. The middle of the bay (y ~ 0) should, according to the Cosine model, show little emission since the magnetic field is approximately tangent along the central portion, i.e. $|90-\theta_i| \sim 0°$, as shown in Fig. 3c. In contrast, the intensity near the middle of the bay (y = 0) is close to the maximum intensity at all vertical locations z.

4 Monte Carlo Modelling - Vertical Distributions

Fig. 5a gives the vertical (with horizontally integration) intensity distributions for D_α, He I and C II emissions from a sequence (58932 - 58944) of identical deuterium neutral-beam heated Supershot discharges with $I_p = 0.8MA$, $B_T = 3.5T$, deuterium NBI power $P_{NBI} \sim 9MW$, $\Lambda \sim 2.1$ and $\bar{n}_e \sim 1.9 \times 10^{19} m^{-3}$. In these discharges, trace helium gas puffing was employed which allowed the He I distribution on the limiter to be measured. These distributions, despite originating under different plasma conditions, are similar to those of Section 3 and demonstrate the general robustness of the experimental distributions to varied plasma conditions.

The vertical distributions in Fig. 5a have been modelled with the LIM Monte Carlo transport code [11]. The code assumes a toroidally symmetric limiter with a circular poloidal profile (as in Fig. 1). The neglect of the toroidal convolutions in the limiter structure in this case are valid since their typical dimension, i.e. ~ 4 mm (see Fig. 2b), are very much smaller than the scrape-off layer dimension at the limiter, i.e. $\lambda_r \sim 5cm$. Test deuteron ions are started on a flux surface 10 cm inside the LCFS (r = 0.70 m) with a uniform poloidal distribution and with parallel velocities of $1.1 \times 10^5 m/s$, corresponding approximately to an ion temperature of 100 eV, which is typical of that measured with the reciprocating Langmuir probe in the boundary plasma. The particle is followed within a plasma grid taking into account random-walk cross-field diffusion and collisionless parallel field motion. The collisionless parallel motion approximates the flow of a background deuterium fluid. (The assumption of collisional-diffusive parallel motion causes only minor changes to the derived distributions.) The particle is followed until it strikes the limiter, either by cross-field or parallel motion.

The deposition pattern on the limiter, following the averaging of 5000 trajectories, is compared with the experimental results in Fig. 5b. To bring out the importance of cross-field transport close to the limiter, three LIM runs are compared here. In the first, cross-field diffusion is spatially uniform throughout the plasma volume at a value of $D = 10 m^2/s$. In the second, cross-field diffusion is reduced close to the limiter ($R < R_0$) to a value of $D = 2 m^2/s$. In the third,

cross-field diffusion is turned off close to the limiter. The third case approximately reproduces the analytic result [10] obtained using the Cosine law. Note the presence of a null at the mid-plane and a double peak structure, in strong contrast to the experimental profiles.

In the first case, with uniform diffusion, although the overall width of the distribution is approximated (as well as the density e-folding distance in the SOL, i.e. from LIM $\lambda_n \sim 4.5cm$), the distribution is essentially constant in the interaction region. A better match between the code result and the experiment is obtained in the second case, where cross-field diffusion is reduced in the region $R < R_0$ but is still finite. In this case, both the overall width of the distribution and the mid-plane intensity level are approximated. A similar spatial variation of the diffusion coefficient was needed in an earlier study [9] to explain the observation in TFTR of long particle confinement times combined with long particle e-folding distances in the SOL. The former implies reduced diffusion close the neutral source near the limiter while the latter implies enhanced diffusion away from the limiter.

The calculated deposition patterns are somewhat narrower than the observed spectroscopic profiles, possibly because of the finite mean free paths of the neutrals, which can be long at the top and bottom regions of the limiter where the SOL plasma density and temperature are low.

5 Monte Carlo Modelling - Horizontal Distributions

In this section we consider the shadow region between adjacent bays and for simplicity concentrate on the midplane region. The geometry is shown in Fig. 2b. The LCFS is assumed to be a straight line whilst the toroidal limiter surface is approximated, to maintain the correct geometry, by an arc of a circle with a radius of 7.4 m.

The horizontal distributions corresponding to the discharges discussed in the last section are given in Fig. 6a. These have also been modelled in a Monte Carlo fashion using a new code, SHADOW. The code, is specifically designed to investigate small shadow regions where finite Larmor radius effects might be important. Particles are started on a flux surface some distance inside the LCFS (a - r = 1 cm) with a Maxwellian distribution of velocities corresponding to parallel and perpendicular ion temperatures, and followed taking into account their Larmor orbits and random-walk cross-field diffusion of the particle's guiding centre. The motion of the particle is assumed to be collisionless and thus neither the parallel nor perpendicular velocities are altered after the initial launch. The particles are followed within the plasma grid until they strike the limiter.

Results for the deposition of particles on the limiter produced by SHADOW appear in Fig. 6 for comparison with experiment. Four cases are shown. In the first two, Fig. 6b, cross-field diffusion is assumed to be spatially uniform at a levels of $D = 2m^2/s$ and $D = 10m^2/s$, corresponding to the values from the last section for $R < R_0$ and $R > R_0$, respectively. An ion temperature of $T_i = 100eV$ is used. Although the derived distributions are not strongly sensitive to the assumed diffusion coefficient, it appears that the smaller value gives better agreement with the experimental distributions, while the larger value gives a distribution which is too broad. Both of these cases have been run with the perpendicular ion temperature increased to 1000 eV to investigate the importance of the finite Larmor radius (not shown). Negligible effect on the resulting distributions was found.

In the final two cases, Fig. 6c, the Cosine model with finite Larmor radius is compared. In these cases, cross-field diffusion is turned off, a flux density e-folding distance of $\lambda_\Gamma = 2mm$ is assumed in the shadow region and the particles are followed to the limiter surface. Again, two plasma temperatures are used to bring out the importance of the Larmor radius, $T_i = 100eV$ and $T_i = 1000eV$. The lower temperature case closely reproduces the analytic Cosine model with zero Larmor radius while in the case with the high ion temperature, the flux distribution on the surface is only slightly affected by the large Larmor orbits, which tend to reduce the flux reaching the middle regions of the limiter. This is due to the scraping-off effect of the surface as the ions move along field lines with their finite orbits.

From the comparison of the SHADOW results with the experimental distributions, it appears that the experiment is best reproduced by the first case in Fig. 6b, where $D = 2m^2/s$ and $T_i = 100eV$. The smaller diffusion coefficient is consistent with that needed to explain the vertical distribution in the last section. This is perhaps surprising considering that in the present case, diffusion over the scale-length of millimetres in close proximity to a material surface is considered, compared with radial scale-lengths of centimetres in the global SOL.

6 Sputtering Yields

Although the mechanisms leading to the emission of D_α, He I and C II photons differ widely, both the vertical and horizontal intensity distributions (Figs. 5a and 6a) for the three species are similar. This is consistent with the sputtering yields for plasma ions being constant across the limiter surface, i.e. independent of the angle between the surface and the field. Unfortunately, at the present time there exists no model in the literature to compare with this experimental finding which is suitable under these conditions of very oblique angles.

7 Discussion

Recently, a number of experiments have investigated the fluxes of particles and power to surfaces at oblique angle in tokamaks. An earlier TFTR study (see [3]) compared the power incident on the original poloidal rail limiter as measured by infrared thermography with that expected assuming only parallel heat transport to the surface; an "anomalous" cross-field heat flow to the surface was invoked to explain the heat deposition pattern observed. On the DITE tokamak [3], it was shown that both the ion and power flux densities incident on a plate which could be inclined at arbitrary angles with respect to the magnetic field did not depend on the angle for $|90-\theta| < 3°$. The Cosine law was found to be approximately obeyed for $|90-\theta| > 3°$. Recently, carbon and beryllium emissions around the JET belt limiters were successfully modelled assuming the Cosine law [12,13], apparently in contradiction to these findings. However, it was shown in these studies that because of the small poloidal dimension of these limiters, the finite mean free paths of sputtered atoms obscured the plasma deposition pattern. On the DIII tokamak [14], the power density incident on the divertor plates was shown to follow the Cosine law down to angles $|90-\theta| \sim 0.5°$, in apparent and unresolved contradiction to the earlier TFTR and DITE results.

In this paper we have demonstrated that ion flow to the TFTR inner-wall bumper limiter does not follow the simple Cosine law when the angle of the field with the surface is very glancing or oblique. This is primarily due to the presence of cross-field particle transport, which becomes important when the flux onto surfaces due to parallel flow is reduced to small levels at oblique angles according to the Cosine law. A more detailed exposition of this process - which involves a two-dimensional funnelling or concentrating effect within the confined plasma - will be published elsewhere [15], including a discussion of the apparently divergent results from the various tokamak studies mentioned above.

In the past the problem of particle and power flow to limiters has been considered either using analytic calculations or by solving the fluid flow equations in two-dimensional geometry. Both approaches have been deficient when the field angle with the surface is oblique. In the analytic case, the two-dimensional flow problem is split into two one-dimensional problems - one of radial transport, whose typical solution is an exponential decay of density (and flux density) in the radial direction in the SOL, followed by a simple mapping of this onto the limiter using the Cosine law. Such an approach is valid under certain limiting conditions, for example, where the angle between the magnetic field and the limiter surface is not oblique, i.e. $|90-\theta| > 3°$, this

typically occurs when the area of the limiter is relatively small compared to the plasma surface area. However, in general, and especially with the large-area limiters in present and future machines, the problem is inherently two-dimensional in nature and such an approach fails. In the case of fluid codes, while two-dimensional geometry is used and cross-field diffusion is allowed for within the plasma, the boundary condition at the plasma-surface interface typically only allows for parallel field exhaust of particles and power to the surface and thus the Cosine law is assumed.

The fact that a significant portion of the ion flow to surfaces at oblique angles is due to cross-field transport has a number of important practical consequences to present and future machines. First, for TFTR it appears from these studies that the wetted area of the limiter, i.e. that area which is sharing particles exhausted from the plasma, is approximately twice that expected based on the simple Cosine model, thus suggesting the limiter can handle nearly twice the input power (assuming no hot spots [16] and that the power distribution is similar to the particle distribution). Second, for TFTR and future machines which make use of very oblique angles to reduce particle and power densities on limiter or divertor tiles, the results of this study suggest that tile alignment is not of critical importance since particle densities are independent of angle under very oblique conditions (assuming no tile edges protrude). The last conclusion is not supported, however, by the recent DIII results on power deposition to the divertor plates [14]. It is therefore planned to attempt similar power deposition measurements on the TFTR bumper limiter.

8 Conclusions

(1) The Cosine law describing the flow of particles to surfaces does not appear to hold for the TFTR bumper limiter where the angle between the magnetic field and the surface is oblique, in agreement with the earlier TFTR and DITE results for $|90-\theta| < 3°$ [3].

(2) The distributions can be explained by considering both parallel and cross-field transport of particles to the limiter.

(3) The cross-field transport of particles appears to behave the same on radial scale-lengths of millimetres in close proximity to the limiter as with diffusion on the scale length of centimetres in the global SOL.

(4) The spatial distributions are consistent with a cross-field diffusion being significantly larger at large major radii ($D = 10m^2/s$ for $R > R_0$) compared with small major radii ($D = 2m^2/s$ for $R > R_0$).

(5) The significant flux reaching the tangency point on the limiter cannot be explained by the finite Larmor orbit of particles.

(6) The similarity of the C II pattern to the D_α and He I distributions suggests that the physical sputtering yields are not dependent on angle within the range $|90 - \theta| < 3°$.

(7) The effect of the cross-field transport to the limiter is to enhance the wetted area of the TFTR limiter by a factor of ~ 2 and to reduce the importance of tile alignment (provided tile edges are protected).

Acknowledgements

This work was supported by U.S. Department of Energy Contract No. DE-AC02-76-CHO-3073, No. DE-AC04-76DP00789 and No. DE-FG05-90ER54091. C S Pitcher and P C Stangeby are grateful for personal support from the Canadian Fusion Fuels Technology Project and to Lorie Sikura for graphics assistance.

References

(1) M Ulrickson, in "Physics of Plasma-Wall Interactions in Controlled Fusion", Eds. D E Post and R Behrisch, NATO ASI Series, Plenum Press, New York (1986).

(2) S A Cohen et al, 13th IAEA Int Conf Contr Fusion Research, (1990) Washington, USA, paper IAEA-CN-53/F-3-3.

(3) G F Matthews, S J Fielding, G M McCracken et al, Plas Phys Contr Fus 32 (1990) 1301.

(4) R T McGrath and J N Brooks, J Nucl Mat 162-164 (1989) 350.

(5) T Hua et al, presented at the 10th Int Conf on PSI in Controlled Fusion Devices (1992) Monterey, USA.

(6) S S Medley, D L Dimock, S Hayes et al, Rev Sci Instrum 56 (1985) 1873.

(7) C S Pitcher, Vacuum Technology Applications and Ion Physics, 38 (1988), 1059.

(8) K Behringer, H P Summers, B Denne, M Forrest and M Stamp, Plas Phys Contr Fus 31 (1989) 2059.

(9) C S Pitcher, P C Stangeby, R V Budny et al, Nucl Fusion 32 (1992) 239.

(10) R V Budny, J Nucl Mat 93/94 (1980) 449.

(11) P C Stangeby, C Farrel, S Hoskins and L Wood, Nucl Fusion 28 (1988) 1945

(12) C S Pitcher, G M McCracken, P C Stangeby and D D R Summers, Proceedings of the 16th European Conference on Controlled Fusion and Plasma Physics, Venice, March 1989, 13B III, 879.

(13) A Hwang, D Elder, D H J Goodall et al, presented at the 10th Int Conf on PSI in Controlled Fusion Devices (1992) Monterey, USA.

(14) G F Matthews, D N Hill and M Ali Mahdavi, Nucl Fusion 31 (1991) 1383.

(15) P C Stangeby, C S Pitcher et al, to be submitted to Nucl Fusion (1992), in preparation.

(16) M Ulrickson, J Nucl Mat 176/177 (1990) 44.

Figure Captions

(1) Schematic cross-section diagram of the TFTR vessel showing the arrangement of the toroidal graphite bumper limiter, the reciprocating Langmuir probe and the periscope viewing system.

(2) Schematic views of bay P of the TFTR toroidal bumper limiter. (A) View along a major radius from the perspective of the camera. The assumed coordinate system and the orientation of the magnetic field are shown. The interaction with the plasma is expected to be most intense in the upper left and low right quadrants of the bay. (B) Cross-section of the limiter through the mid-plane showing the regular toroidal convolution in the limiter shape.

(3) Contour maps on the bumper limiter at bay P above the mid-plane for a deuterium Ohmic discharge with $I_p = 1.4MA$, $B_T = 4T$ and $\overline{n}_e = 3x10^{19}m^{-3}$. (A) The experimental D_α normalized intensity. (B) The expected (normalized) flux density of deuterons striking the limiter assuming the Cosine law with shadowing by neighbouring bays and a particle flux e-folding distance at the outside mid-plane of $\lambda_\Gamma = 3.0cm$. (C) Angles between the surface and the magnetic field, i.e. $|90-\theta|$, where θ is the angle between the field and the surface normal.

(4) Comparison of the experimental normalized D_α intensity distributions with the Cosine model from Fig. 3. (A) The vertical distribution obtained by horizontal integration across the bay. (B) The horizontal distribution at a vertical height of z = 0.5 m.

(5) (A) The experimental normalized D_α, He I and C II vertical intensity distributions (with horizontal integration) in a Supershot discharge with $I_p = 0.8MA$, $B_T = 3.5T$, deuterium NBI power P_{NBI}~$9MW$, Λ~2.1 and $\overline{n}_e$~$1.9x10^{19}m^{-3}$. (B) The normalized deposition pattern determined by LIM assuming the following spatial variation of cross-field diffusion coefficient ($R < R_0$, $R > R_0$), (10, 10), (2, 10) and (0, 10) m^2/s.

(6) (A) The experimental normalized D_α, He I and C II horizontal intensity distributions at the mid-plane in the same conditions as Fig. 5. (B) The normalized deposition pattern determined by SHADOW assuming cross-field diffusion coefficients of $D = 2m^2/s$ and $D = 10m^2/s$. (C) The deposition pattern determined by SHADOW assuming the Cosine law, i.e. with no cross-field diffusion and a particle flux e-folding distance in the shadow region of $\lambda_\Gamma = 2mm$ and ion temperatures of $T_i = 100eV$ and $T_i = 1000eV$.

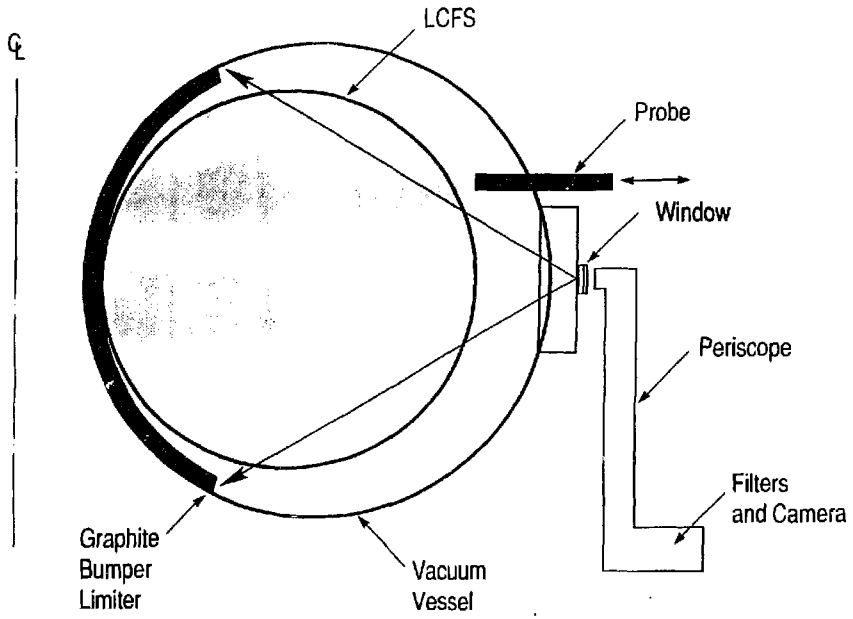
LCFS
Probe
Window
Periscope
Filters
and Camera
Graphite
Bumper
Limiter
Vacuum
Vessel

Fig. 1

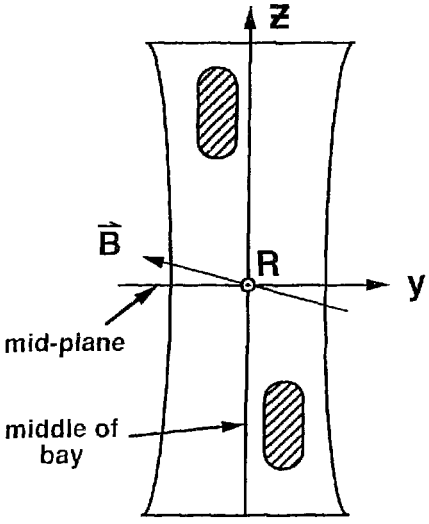

(A)

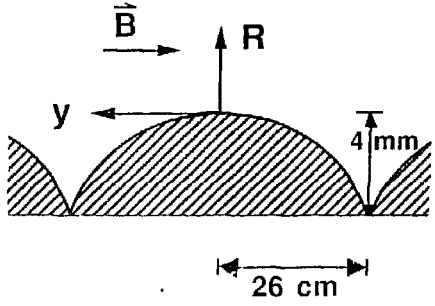

(B)

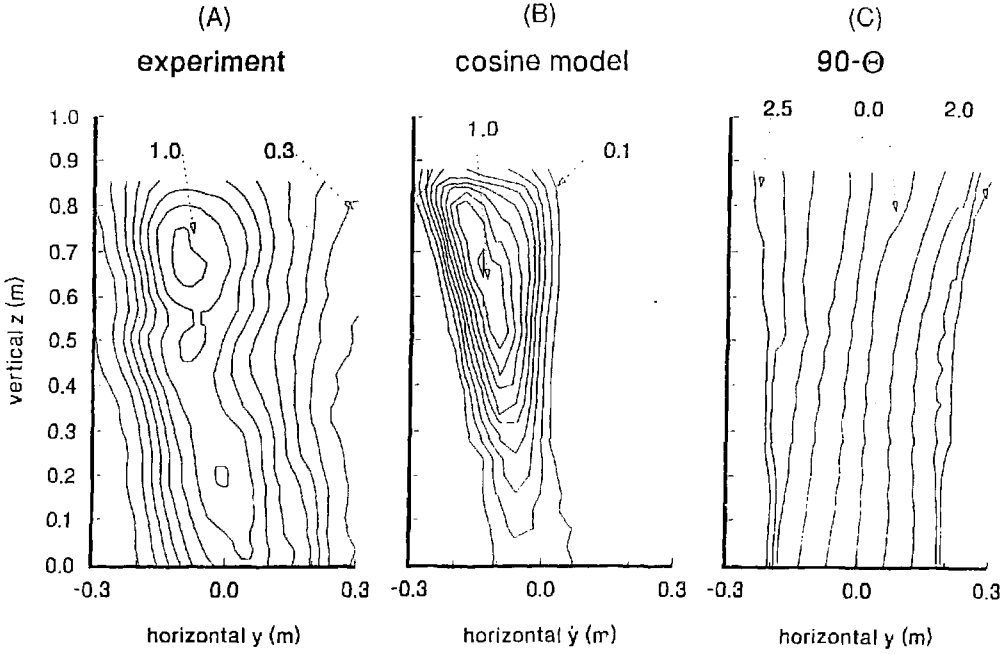
(A)
experiment
(B)
cosine model
(C)
90-Θ
vertical z (m)
1.0
0.9
0.8
0.7
0.6
0.5
0.4
0.3
0.2
0.1
0.0
1.0
0.3
1.0
0.1
2.5
0.0
2.0
-0.3
0.0
0.3
horizontal y (m)
horizontal y (m)
horizontal y (m)

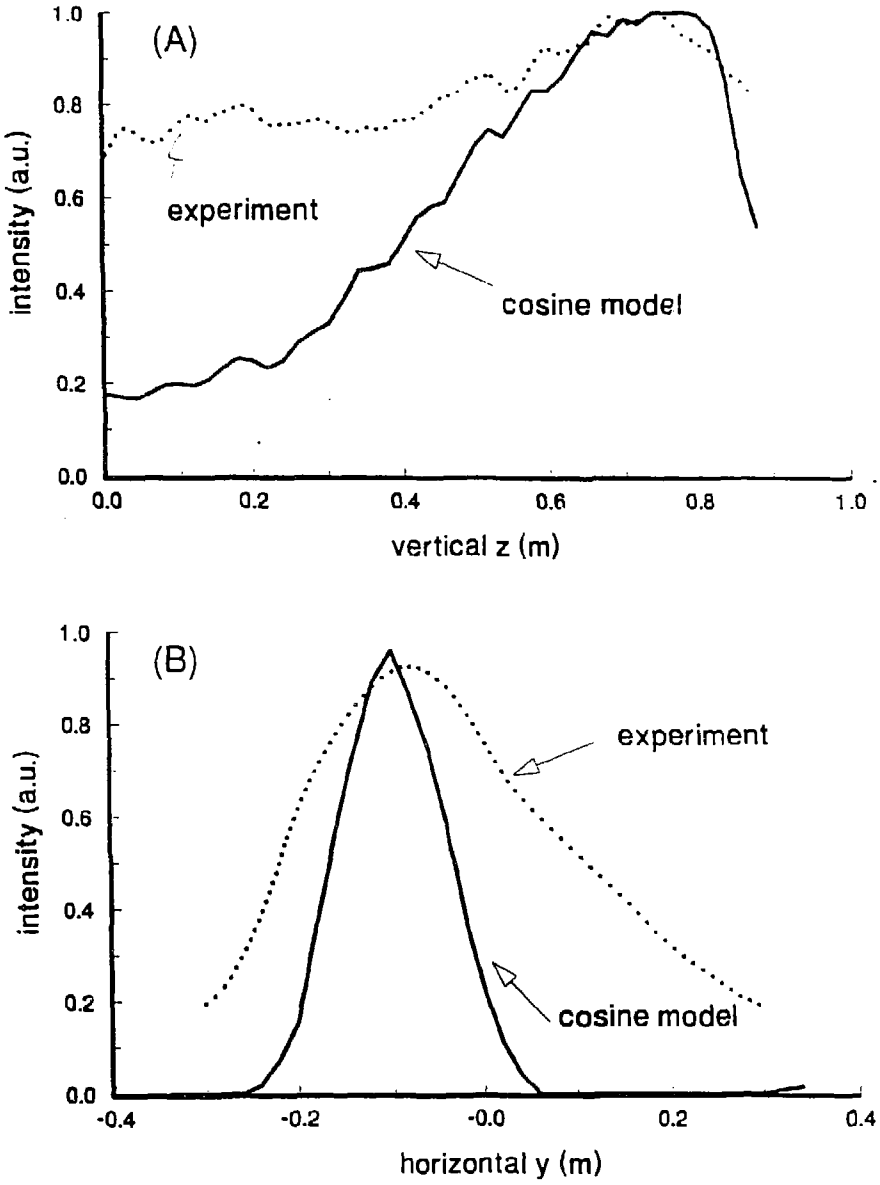
(A)
intensity (a.u.)
1.0
0.8
0.6
0.4
0.2
0.0
experiment
cosine model
0.0
0.2
0.4
0.6
0.8
1.0
vertical z (m)
(B)
intensity (a.u.)
1.0
0.8
0.6
0.4
0.2
0.0
experiment
cosine model
-0.4
-0.2
-0.0
0.2
0.4
horizontal y (m)

Fig. 4

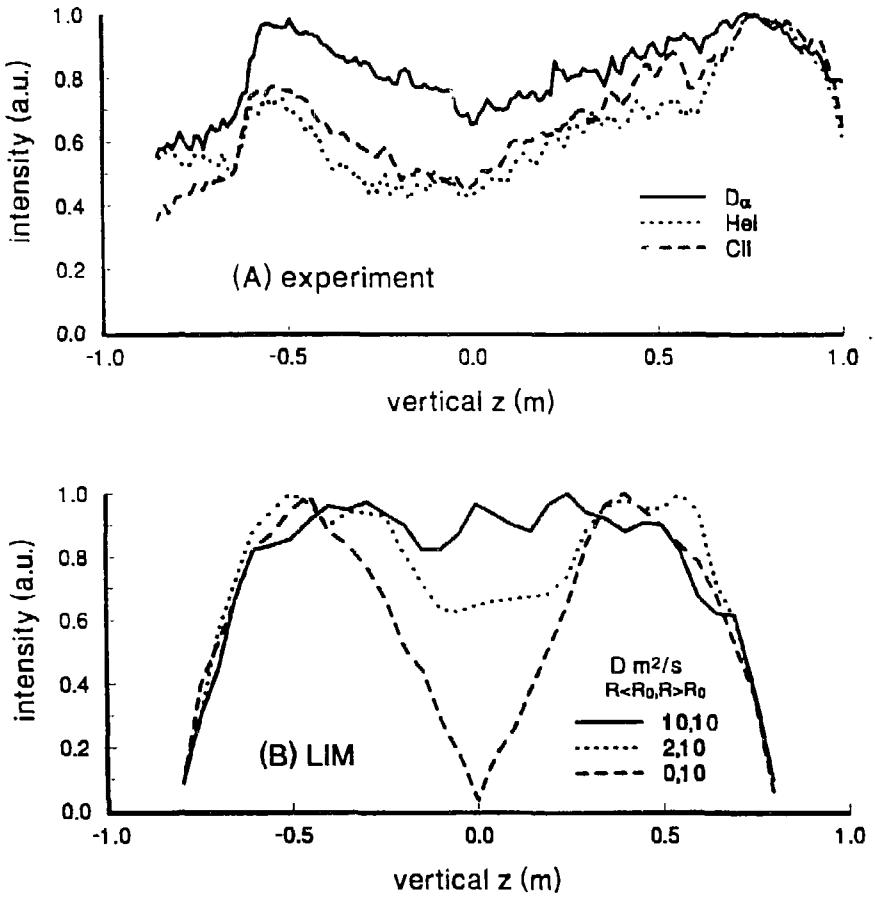
intensity (a.u.)
1.0
0.8
0.6
0.4
0.2
0.0
-1.0
-0.5
0.0
0.5
1.0
vertical z (m)
(A) experiment
Dα
HeI
CII
intensity (a.u.)
(B) LIM
D m²/s
R<R0,R>R0
10,10
2,10
0,10
vertical z (m)

Fig. 5

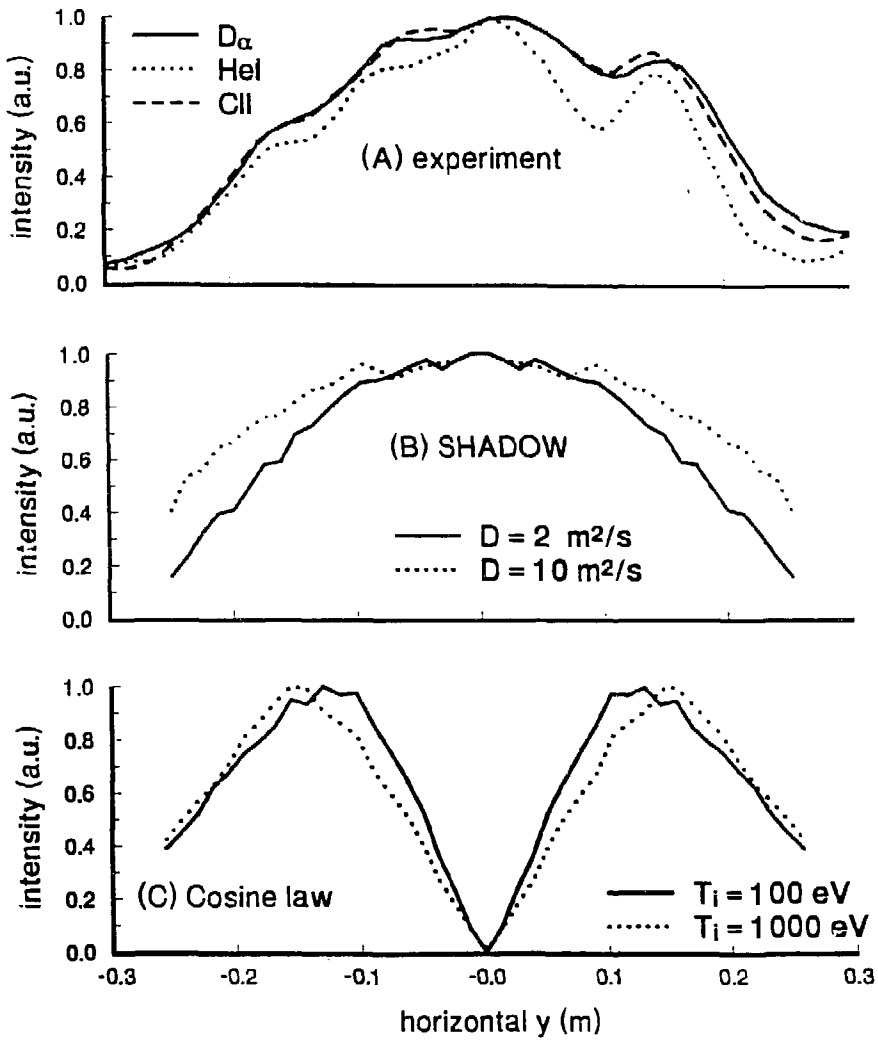
1.0
0.8
0.6
0.4
0.2
0.0
intensity (a.u.)
Dα
HeI
CII
(A) experiment
(B) SHADOW
D = 2 m²/s
D = 10 m²/s
(C) Cosine law
Ti = 100 eV
Ti = 1000 eV
-0.3
-0.2
-0.1
-0.0
0.1
0.2
0.3
horizontal y (m)

Fig. 6

EXTERNAL DISTRIBUTION IN ADDITION TO UC-420

Dr. F. Paoloni, Univ. of Wollongong, AUSTRALIA
Prof. M.H. Brennan, Univ. of Sydney, AUSTRALIA
Plasma Research Lab., Australian Nat. Univ., AUSTRALIA
Prof. I.R. Jones, Flinders Univ, AUSTRALIA
Prof. F. Cap, Inst. for Theoretical Physics, AUSTRIA
Prof. M. Heindler, Institut für Theoretische Physik, AUSTRIA
Prof. M. Goossens, Astronomisch Instituut, BELGIUM
Ecole Royale Militaire, Lab. de Phy Plasmas, BELGIUM
Commission-European, DG. XII-Fusion Prog., BELGIUM
Prof. R. Boucique, Rijksuniversiteit Gent, BELGIUM
Dr. P.H. Sakanaka, Instituto Fisica, BRAZIL
Instituto Nacional De Pesquisas Espaciais-INPE, BRAZIL
Documents Office, Atomic Energy of Canada Ltd., CANADA
Dr. M.P. Bachynski, MPB Technologies, Inc., CANADA
Dr. H.M. Skarsgard, Univ. of Saskatchewan, CANADA
Prof. J. Teichmann, Univ. of Montreal, CANADA
Prof. S.R. Sreenivasan, Univ. of Calgary, CANADA
Prof. T.W. Johnston, INRS-Energie, CANADA
Dr. R. Bolton, Centre canadien de fusion magnétique, CANADA
Dr. C.R. James,, Univ. of Alberta, CANADA
Dr. P. Lukac, Komenskeho Universzita, CZECHO-SLOVAKIA
The Librarian, Culham Laboratory, ENGLAND
Library, R61, Rutherford Appleton Laboratory, ENGLAND
Mrs. S.A. Hutchinson, JET Library, ENGLAND
Dr. S.C. Sharma, Univ. of South Pacific, FIJI ISLANDS
P. Mähönen, Univ. of Helsinki, FINLAND
Prof. M.N. Bussac, Ecole Polytechnique,, FRANCE
C. Mouttet, Lab. de Physique des Milieux Ionisés, FRANCE
J. Radet, CEN/CADARACHE - Bat 506, FRANCE
Prof. E. Economou, Univ. of Crete, GREECE
Ma. C. Rinni, Univ. of Ioannina, GREECE
Dr. T. Mual, Academy Bibliographic Ser., HONG KONG
Preprint Library, Hungarian Academy of Sci., HUNGARY
Dr. B. DasGupta, Saha Inst. of Nuclear Physics, INDIA
Dr. P. Kaw, Inst. for Plasma Research, INDIA
Dr. P. Rosenau, Israel Inst. of Technology, ISRAEL
Librarian, International Center for Theo Physics, ITALY
Miss C. De Palo, Associazione EURATOM-ENEA , ITALY
Dr. G. Grosso, Istituto di Fisica del Plasma, ITALY
Prof. G. Rostangni, Istituto Gas Ionizzati Del Cnr, ITALY
Dr. H. Yamato, Toshiba Res & Devel Center, JAPAN
Prof. I. Kawakami, Hiroshima Univ., JAPAN
Prof. K. Nishikawa, Hiroshima Univ., JAPAN
Director, Japan Atomic Energy Research Inst, JAPAN
Prof. S. Itoh, Kyushu Univ., JAPAN
Research Info. Ctr., National Instit. for Fusion Science, JAPAN
Prof. S. Tanaka, Kyoto Univ., JAPAN
Library, Kyoto Univ., JAPAN
Prof. N. Inoue, Univ. of Tokyo, JAPAN
Secretary, Plasma Section, Electrotechnical Lab., JAPAN
S. Mori, Technical Advisor, JAERI, JAPAN
Dr. O. Mitarai, Kumamoto Inst. of Technology, JAPAN
J. Hyeon-Sook, Korea Atomic Energy Research Inst., KOREA
D.I. Choi, The Korea Adv. Inst. of Sci. & Tech., KOREA
Prof. B.S. Liley, Univ. of Waikato, NEW ZEALAND
Inst of Physics, Chinese Acad Sci PEOPLE'S REP. OF CHINA
Library, Inst. of Plasma Physics, PEOPLE'S REP. OF CHINA
Tsinghua Univ. Library, PEOPLE'S REPUBLIC OF CHINA
Z. Li, S.W. Inst Physics, PEOPLE'S REPUBLIC OF CHINA
Prof. J.A.C. Cabral, Instituto Superior Tecnico, PORTUGAL
Dr. O. Petrus, AL I CUZA Univ., ROMANIA
Dr. J. de Villiers, Fusion Studies, AEC, S. AFRICA
Prof. M.A. Hellberg, Univ. of Natal, S. AFRICA
Prof. D.E. Kim, Pohang Inst. of Sci. & Tech., SO. KOREA
Prof. C.I.E.M.A.T, Fusion Division Library, SPAIN
Dr. L. Stenflo, Univ. of UMEA, SWEDEN
Library, Royal Inst. of Technology, SWEDEN
Prof. H. Wilhelmson, Chalmers Univ. of Tech., SWEDEN
Centre Phys. Des Plasmas, Ecole Polytech, SWITZERLAND
Bibliotheek, Inst. Voor Plasma-Fysica, THE NETHERLANDS
Asst. Prof. Dr. S. Cakir, Middle East Tech. Univ., TURKEY
Dr. V.A. Glukhikh,Sci. Res. Inst. Electrophys.l Apparatus, USSR
Dr. D.D. Ryutov, Siberian Branch of Academy of Sci., USSR
Dr. G.A. Eliseev, I.V. Kurchatov Inst., USSR
Librarian, The Ukr.SSR Academy of Sciences, USSR
Dr. L.M. Kovrizhnykh, Inst. of General Physics, USSR
Kernforschungsanlage GmbH, Zentralbibliothek, W. GERMANY
Bibliothek, Inst. Für Plasmaforschung, W. GERMANY
Prof. K. Schindler, Ruhr-Universität Bochum, W. GERMANY
Dr. F. Wagner, (ASDEX), Max-Planck-Institut, W. GERMANY
Librarian, Max-Planck-Institut, W. GERMANY
Prof. R.K. Janev, Inst. of Physics, YUGOSLAVIA